

UNIVERSITY OF OXFORD

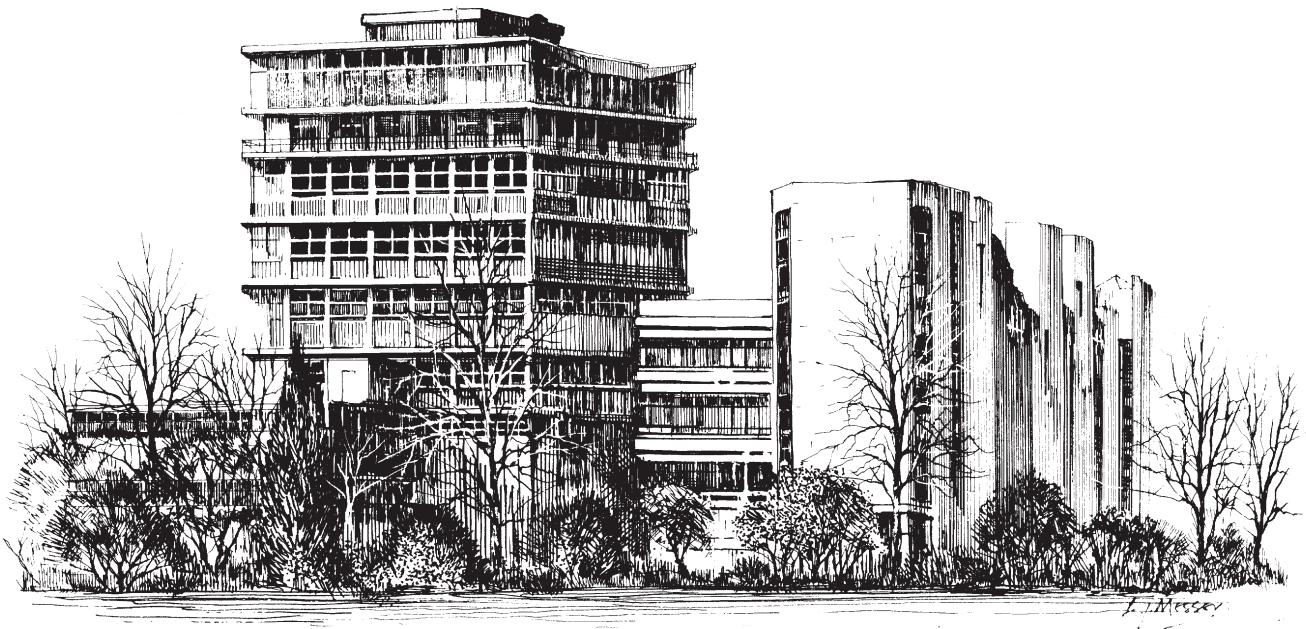
Department of Engineering Science

Parks Road

Oxford



Report



OUEL 2302/08

Bending-Buckling Interaction: Investigation of this Failure Mechanism of Pile Foundations in Seismically Liquefiable Deposits

by

Suresh R Dash¹
Dr. Subhamoy Bhattacharya²
Dr. Anthony Blakeborough³

REPORT NO. OUEL 2302/08

(Part of this work has been accepted for publication in the Journal of Soil Dynamics and Earthquake Engineering, Elsevier Ltd)



University of Oxford
Department of Engineering Science
Parks Road, Oxford, OX1 3PJ, UK
Tel. 01865 273162/283300
Fax. 01865 283301
Email: civil@eng.ox.ac.uk
<http://www-civil.eng.ox.ac.uk/>

¹Dept. of Engineering Science, University of Oxford, UK. E-mail: Suresh.Dash@eng.ox.ac.uk

²Dept. of Civil Engineering, University of Bristol, UK. E-mail: S.Bhattacharya@bristol.ac.uk

³Dept. of Engineering Science, University of Oxford, UK. E-mail: Tony.Blakeborough@eng.ox.ac.uk

Bending-Buckling Interaction: Investigation of this Failure Mechanism for Pile Foundations in Seismically Liquefiable Deposits

Suresh R Dash ¹ Subhamoy Bhattacharya ² Anthony Blakeborough ³

Abstract

This report investigates the importance of bending-buckling interaction in seismic design of piles in liquefiable soils. Recent studies have identified a possible mechanism of failure of piles in liquefiable soils; i.e., piles designed for bending and buckling separately may fail due to their combined effect. Fifteen cases of pile performance in past earthquakes have been assessed. In most of these cases bending-buckling interaction appears to be the cause of pile failure. One of the well documented case histories, i.e., the Showa bridge pile failure in 1964 Niigata earthquake, has been analyzed in detail. A pseudo-static analysis has been performed where the pile is modelled as a Beam on Nonlinear Winkler Foundation (BNWF). Six possible methods of analysis for piles subjected to lateral and axial loads are investigated, three force based and three displacement based. Three out of six analysis cases could not predict the failure of the piles subjected to only bending (i.e., Lateral loads only). Also, the buckling analysis showed that the Showa bridge pile was safe against Euler buckling. Two out of three cases those could not predict failure were reanalyzed for combined bending and buckling (i.e., Lateral and axial loads acting simultaneously). This bending-buckling analysis showed more realistic behaviour of pile response and could predict the pile failure. However, the actual reason for Showa Bridge pile failure may be a combination of various mechanisms.

¹Dept. of Engineering Science, University of Oxford, UK.

²Dept. of Civil Engineering, University of Bristol, UK.

³Dept. of Engineering Science, University of Oxford, UK.

1 Introduction

The collapse of piled structures is observed after many strong earthquakes, despite the fact that a large factor of safety (against bending due to lateral loads and axial capacity) is employed in their design, see for example Bhattacharya and Madabhushi (2008). This suggests that the bending moments or shear forces that are experienced by the piles exceed the bending or shear carrying capacity of the pile section. Most design codes apparently provide a high margin of safety to these mechanisms using partial safety factors, yet pile failures in areas of seismic liquefaction frequently occur. Currently, piles in liquefiable soils are designed as beams to resist bending failure from lateral loads due to the inertia of the structure and/or slope movement (lateral spreading). Bhattacharya (2003) showed that the overall factor of safety against plastic yielding of a typical concrete pile can range between 4 and 8. This is due to the multiplication of partial safety factors on load (1.5), material (1.5 for concrete), fully plastic strength factor ($Z_P/Z_E = 1.67$ for a circular section) and practical factors such as minimum reinforcement requirements or minimum number of reinforcement bars. This implies that the actual bending moment or shear force experienced by the piles are possibly 4 to 8 times those predicted by their design methods. It may be concluded that either the design methods are not consistent with the physical mechanisms that govern the failure, or the seismic forces are severely underestimated.

Pile foundations in liquefiable soils subjected to seismic shaking may fail either due to a) excessive settlement, b) shear or c) bending. These mechanisms are well understood and the codes of practice use them to set design guidelines. Of these mechanisms, bending due to liquefaction induced lateral spreading of the ground is often regarded as the root cause of many pile foundation failures during earthquakes, see for example (Hamada (1992a), Hamada (1992b), Ishihara (1997), Tokimatsu et al. (1998), Goh and O'Rourke (1999), Abdoun and Dobry (2002) and Finn and Fujita (2002)).

Recently, buckling instability has been cited as another possible mechanisms of pile failure in liquefiable soils (Bhattacharya (2003), Bhattacharya et al. (2004), Knappett and Madabhushi (2005), Kimura and Tokimatsu (2005), Shanker et al. (2007) etc.). The proposed mechanism is that, during liquefaction, the pile suffers a significant loss of lateral support

in the liquefied zone. If the axial load is very high (i.e., near to the critical buckling load), buckling instability of end-bearing pile may occur promoted by the actions of lateral loads and/or imperfections. Bhattacharya et al. (2008) considers this as an omission in seismic pile design. Dash and Bhattacharya (2007) summarized various mechanisms of pile failure during earthquakes. They have grouped shear, bending and buckling mechanisms as '*Limit State of Collapse*', as these are associated with the structural failure of piles, e.g., formation of plastic hinges or cracks. On the other hand, excessive settlement of pile is regarded as the '*serviceability limit state criteria*' which can occur due to the loss of shaft resistance of piles in soft soils during earthquakes and may lead the supported structure to sink or tilt. This form of failure may happen if the pile is not sufficiently embedded in competent soil below the liquefiable soils. In some cases the pile tip may rest in the liquefiable zone. This situation may pose a threat to the overall stability of the pile supported structure in a major seismic event. This form of failure has been explored through the study of the Kandla Port and Customs Office Tower failure during 2001 Bhuj Earthquake (Dash et al. 2009).

Though the two major Limit State of Collapse pile failure mechanisms, bending (due to lateral inertia or lateral soil pressure) and buckling (due to axial load), have been studied in detail separately, little has been reported on their interactions. This report thus investigates the bending-buckling interaction of the pile foundation in a seismically liquefiable soil deposit using a case study.

2 Current understanding of pile failure in liquefiable soil

2.1 Review of some codes of practice

Figure 1 illustrates the current understanding of failure of piles in liquefiable soils. This hypothesis is based on the bending mechanism of failure. Here, the design codes compute the bending moments in piles caused by either lateral spreading of the ground or inertia from the superstructure or a combination of both.

The Japanese Road Association (JRA 2002), for example, advises engineers to design piles against bending failure assuming that the lateral load applied by the liquefied soil during lateral spreading is 30% of the total overburden pressure at the depth of consideration (Figure

1). This criteria will be detailed in section 5.5.1 of this report.

Eurocode (1998) EC 8, for example, advises to design piles against bending due to inertia and kinematic forces arising from the deformation of the surrounding soil recommending that piles should be designed to remain elastic, but the sections at the pile cap and at the interfaces between layers of soil with markedly different properties should have the capacity to form plastic hinges. Eurocode (1998), EC 8:part 5, clause 5.4.2, suggests that the lateral resistance offered by the soil layers susceptible to liquefaction should be ignored.

Other codes, such as NEHRP code (2000) and Indian Code (IS-1893 (2000)) also focus on the design methodology based on the bending strength of the pile. In summary, the current understanding of pile design in codes of practice simply treats piles as beam elements and the lateral loads from structural inertia and/or soil movement cause bending failure of the pile.

Apart from the codes of practice, there are other published procedures that proposes design criteria for piles subjected to seismic loads. For example, Ishihara (1997) noted that during the earthquake soil liquefaction starts approximately at the time of occurrence of peak ground acceleration. He argues that since the seismic motion has already passed its peak, subsequent shaking will be less intense, so that the lateral inertia force applied by the superstructure will not be significant. Therefore, the effects of inertia of the superstructure on the pile response are considered separately and are not combined with the lateral spreading effects. Hamada (2000) mentioned that permanent displacement of non-liquefied soil overlying the liquefied soil is a governing factor for pile damage. A similar conclusion has also been stated by Berrill et al. (2001). Further to this, Tokimatsu et al. (2005) and Tokimatsu and Suzuki (2005) carried out large scale shaking table tests of pile groups in dry and saturated sands and suggested the required conditions and methodology to combine inertial and kinematic loads for piles subjected to seismic loads as follows.

1. When natural period of structure (T_b) > natural period of ground (T_g)

$$M_p = \sqrt{M_i^2 + M_k^2} \quad (1)$$

2. When natural period of structure (T_b) < natural period of ground (T_g)

$$M_p = M_i + M_k \quad (2)$$

Where, M_p = Peak bending moment in pile, M_i = Bending moment in pile due to inertia of superstructure, and M_k = Bending moment in pile due to kinematic loads.

Though the major discussion in the literature is either analysing the piles separately for inertia and lateral spreading or combining them to obtain peak design bending moments for design, the additional bending moment in the pile due to the axial load effects (i.e., *P-delta* effect) and the associated failure mechanism is the main focus of this report. In other words, the importance is given to the necessary incorporation of buckling failure mechanism in the existing bending design framework. It is often suggested that liquefied soil can generate considerable lateral resistance if subjected to shearing due to suppressed dilation. The role of this lateral resistance in resisting buckling of long slender piles is explored in the next section.

2.2 Resistance of liquefied soil to avoid pile buckling

Based on the recent experimental studies, both model tests (laboratory scale and full scale) and element tests (e.g., Takahashi (2002), Wilson et al. (1998), Rollins et al. (2005) and Yasuda et al. (1999)), it may be inferred that liquefied soil can offer significant lateral resistance to a pile i.e. it can regenerate considerable shear strength if it is subjected to ongoing undrained shear strains. Element testing on liquefied soil shows that for a medium dense Toyoura sand (53.9%), shear resistance of liquefied soil develops at about 10% shear strain Yasuda et al. (1999). The origin of this lateral resistance to a pile has been hypothesised due to suppressed dilation of liquefied soil. Takahashi (2002) carried out Experimental work to study the lateral resistance of piles in a liquefied soil, where the pile was modelled as a buried cylinder that could be pushed laterally through liquefied soil. The displacement rate of the cylinder varied from 1mm/sec to 100mm/sec. The test results showed that the initial resistance to movement is negligible at all rates of loading but after a certain amount of displacement the lateral resistance was mobilised. Also, through the analysis of centrifuge

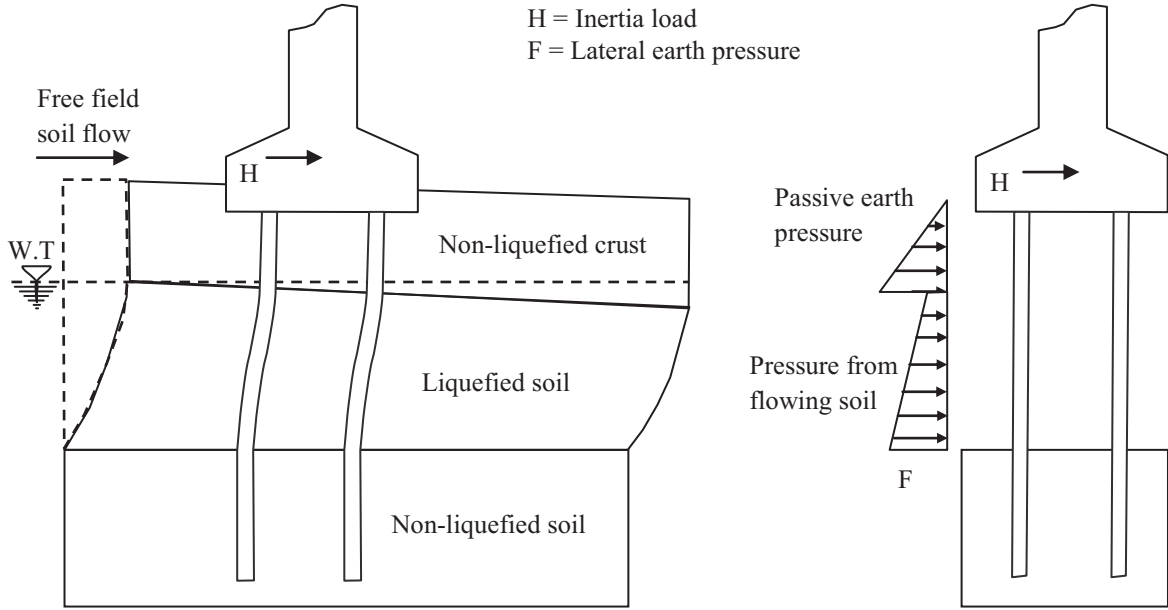


Figure 1. Current understanding of pile failure.

tests, Bhattacharya (2003) showed that the liquefied soil cannot prevent the initiation of buckling in an initially straight pile, however, it may experience some secondary support while going through large deformation (at about 0.3times the diameter of pile).

3 Bending-buckling interaction

To design pile foundations for bending and buckling requires different approaches. Pure bending is a stable mechanism as long as the pile is elastic, i.e., if the lateral load is withdrawn, the pile returns to its initial configuration. This failure mode depends on the bending strength (moment at first yield, M_y , and plastic moment capacity, M_p) of the pile. Buckling, however, represents a sudden instability of the pile, when the axial load in pile reaches the critical buckling load (P_{cr}).

In reality, piles are subjected to both axial and lateral loads during an earthquake and hence act like beam-column members. The presence of the axial load causes lateral unstiffening of the member. If the axial load reaches the critical value, all lateral stiffness is lost and the beam cannot support any further increase in lateral and/or axial load. As axial load approaches the critical value, the loss of lateral stiffness can cause the beam to deflect many times more than it would deflect without the axial load. The ensuing large deflection of the

beam may then induce plasticity in the beam resulting in an early failure. This interaction is generally referred to as P-delta effect in the structural engineering design. Stability analysis of elastic columns (Timoshenko and Gere 1961) shows that the lateral deflection (y_0) due to lateral loads is amplified in the presence of axial load (P) producing a final deflection of pile (y) as given in equation 3. The term ' y/y_0 ' is referred to as the 'Buckling amplification factor (BAF)' which varies for different values of the critical axial force which in turn depends on the boundary conditions of the pile.

$$\frac{y}{y_0} = BAF = \frac{1}{\left(1 - \frac{P}{P_{cr}}\right)} \quad (3)$$

Figure 2 shows a schematic of the effect of bending-buckling interaction on the response of a pile foundation, where the axially loaded pile is subjected to lateral spreading. The figure demonstrates the pile head deflection at three levels of axial loading such as: a) no axial load ($P = 0$), b) axial load at 50% of buckling load ($P = P_{cr}/2$), and c) axial load close to buckling load ($P \approx P_{cr}$). As the axial load increases, the pile head deflection and pile bending moment also increase. When the axial load is close to the buckling load, the bending moment amplification factor becomes very high, which leads the bending moment in pile to reach its plastic moment capacity, M_p , at a lower value of lateral load. The sudden rise in pile head deflection demonstrates the failure point of the pile where bending moment reaches M_p and pile continues to deflect without any additional loading. The similar pattern of bending-buckling interaction can also be possible when the axial loaded piles in level ground subjected to inertia loading. When both inertia and lateral spreading act together and contribute to the lateral loading of pile, the pile may deflect at a larger rate for the same axial load. Fifteen case histories of pile performance in past earthquakes has been studied in the following section to investigate the significance of the bending-buckling interaction.

4 Study of 15 case histories

There are number of cases of seismic performance of pile-supported structures in liquefied soils reported in the literature. Bhattacharya et al. (2008) reported fifteen well documented case histories of how piles performed during the earthquakes. Table 1 summarizes the data

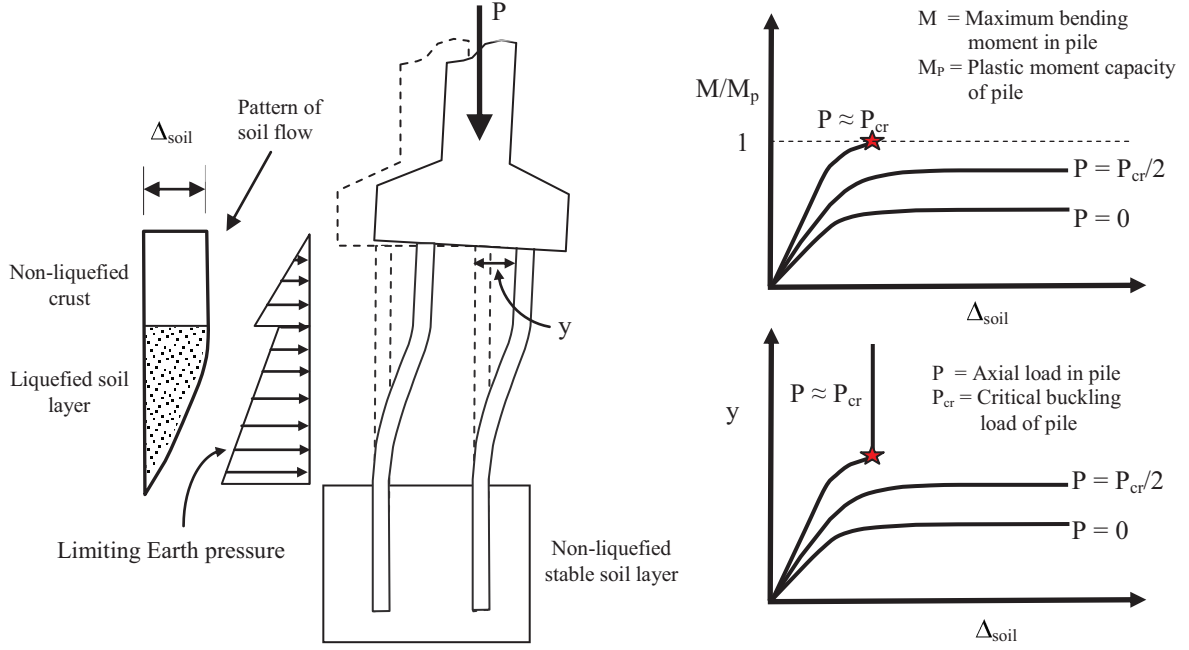


Figure 2. Schematic showing the effect of bending-buckling interaction on the response of pile foundation.

of these case histories. In six of the cases the foundations survived, while in other cases there was severe damage to the piles. For each of the cases, the following parameters were estimated.

1. Critical buckling load of the pile (P_{cr}): This was calculated using the unsupported length of the pile in liquefied soil. The value of P_{cr} depends on the lateral stiffness (EI) and effective length (L_{eff}) of pile. The definition of L_{eff} of pile can be found in Bhattacharya et al. (2004) and Bhattacharya and Madabhushi (2008).
2. Axial load on pile (P): This has been calculated by conventional geotechnical pile capacity calculation. It is essentially the sum of side friction and end bearing capacity of the surrounding soil divided by an appropriate factor of safety. However, it need to be mentioned that the actual load on pile during the earthquake is very difficult to evaluate with the limited information available. Hence the pile capacity calculated by the conventional method is used in this study.

Figure 3 plots the ratio of axial load of the pile to the critical buckling load (P/P_{cr}) for the case histories. The figure shows, with one exception (Case M), the piles having an axial

Table 1. Details of the 15 case histories studied.

Sl.	Case History	Pile details	L_0^* (m)	L_{eff} (m)	P (MN)	P_{cr} (MN)	P/ P_{cr}	**Performance
A	10 storey-Hokuriku building, Hamada (1992a)	0.4m dia RCC	5	5	0.77	12.4	0.062	Good
B	Landing bridge, Berrill et al (2001)	0.4m square PSC	4	2	0.62	139	0.004	Good
C	Hanshin expressway pier, Ishihara (1997)	1.5m dia RCC	15	15	14	272	0.051	Good
D	LPG tank 101, Ishihara (1997)	1.1m dia RCC	15	15	4.1	79	0.052	Good
E	Kobe Shimim hospital, Soga (1997)	0.66m dia steel tube	6.2	6.2	3	91	0.033	Good
F	American Park, Kobe, 14 Story Building under construction, Tokimatsu et al (1996)	2.5m dia RCC	12.2	9.15	18.5	5658	0.003	Good
G	N.H.K building, Hamada (1992a)	0.35m dia RCC	10	20	0.43	0.45	0.956	Poor
H	NFCH building, Hamada (1992a)	0.35m dia RCC hollow	8	16	0.29	0.63	0.460	Poor
I	Yachiyo Bridge, Hamada (1992a)	0.3m dia RCC	8	16	0.34	0.39	0.872	Poor
J	Gaiko Ware House, Hamada (1992a)	0.6m dia PSC hollow	14	28	1.47	1.61	0.913	Poor
K	4 storey fire house, Tokimatsu et al (1996)	0.4m dia PSC	18	18	0.89	0.96	0.927	Poor
L	3 storied building at Kobe university, Tokimatsu et al (1998)	0.4m dia PSC	16	16	0.72	1.02	0.706	Poor
M	Elevated port liner railway, Soga (1997)	0.6m dia RCC	12	12	1.38	10.92	0.126	Poor
N	LPG tank -106&107, Ishihara (1997)	0.3m dia RCC hollow	15	15	0.46	0.38	1.211	Poor
O	Showa bridge, Hamada (1992a)	0.6m dia steel tube.	21.4	42.8	0.74	0.985	0.751	Poor
<p>Note: * L_0 = Unsupported length of pile (pile in liquefied soil is also considered unsupported) ** Good and Poor performances are defined by means of the damage by the respective researchers as referenced.</p>								

load of about $0.5P_{cr}$ or higher failed. Case N, where the axial load in pile is higher than the critical buckling load during liquefaction, is a failure that can be explained by buckling instability alone. In some cases (i.e., H and M), however, the axial load is very low and the buckling amplification factor is correspondingly low. These cases can be considered as the cases that failed primarily in bending or shear due to lateral loads as all the cases considered are on laterally spreading soil. For the remaining six cases (i.e., G, I, J, K, L and O), the

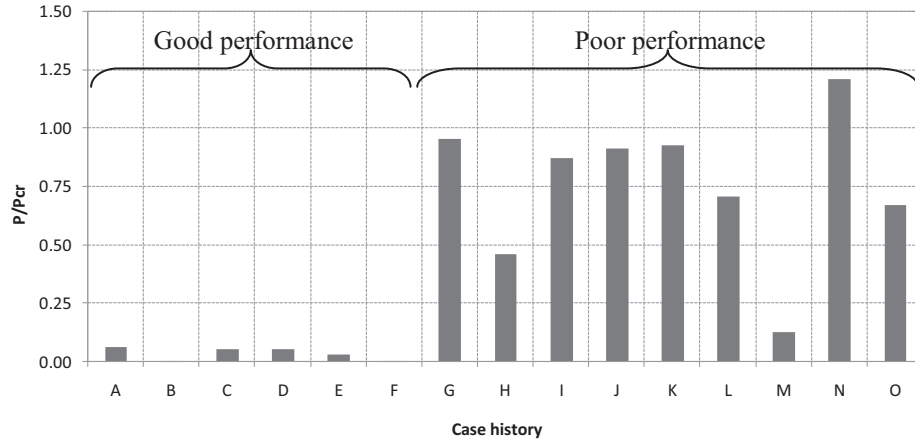


Figure 3. Case histories of pile performance in some major earthquakes.

Table 2. Probable cause of pile failure of the case histories studied

Probable cause of pile failure	Case history number
Bending or shear	M, H
Buckling	N
Bending-buckling interaction	G, I, J, K, L, O

axial load is considerably high proportion of the critical buckling load, which corresponds to a very high value of buckling amplification factor. Hence, it is hypothesized that even with a small lateral loading these piles could have mobilised its plastic moment capacity and failed. These six cases establish the possibility of bending-buckling interaction as a failure mechanism. Though the importance is given to bending-buckling interaction in this report, shear failure in some of these failure cases may not be fully ignored. For example, shear failure may become significant particularly for hollow piles, for example NFCH building (case G). Table 2 summarizes the possible failure mechanisms of these case studies. Of these, case O, the Showa Bridge failure has been investigated in detail following with a numerical model to study, specifically, the bending-buckling interaction.



Figure 4. Collapse of the Showa Bridge after 1964 Niigata earthquake.(Source: NISEE)

5 Numerical study of Showa Bridge pile failure

The failure of Showa Bridge during the 1964 Niigata earthquake as shown in Figure 4 (NISEE) has received significant attention from the research community because of the following three reasons.

1. The bridge collapsed just one month after construction, and had steel tubular piles. This ensures less uncertainty of material strength as degradation of piles due to corrosion is not expected.
2. The shape of the pile after failure and the soil profile is also available from post earthquake investigation (Figure 5).
3. This case history is well documented in many technical papers and reports; see for example Takata et al. (1965), Fukuoka (1966), Iwasaki (1984), Hamada (1992a), Ishihara (1993), (Yoshida et al. 2007), (Kramer 1996), Yoshida et al. (2007).

This case history has been used extensively by researchers to illustrate the effects of lateral spreading on pile foundations, see for example Dobry and Abdoun (2001), Hamada (1992a), Ishihara (1993), Kramer (1996), etc. However, Bhattacharya et al. (2005) demonstrated that the lateral spreading of the soil cannot fully explain the mode of failure of the bridge. This example is used in the present study to investigate the importance of bending-buckling

interaction of piles in liquefiable soils. It must be mentioned here that the exercise is not to ascertain the actual reason for failure, but to show the importance of bending-buckling interaction for piles in liquefiable soils. This also aims to critically study the available methods of analysis.

5.1 Post earthquake observations

During the 1964 Niigata earthquake, the Showa Bridge site was subjected to extensive liquefaction and lateral spreading. After the earthquake, five of the twelve spans had fallen down (Figure 4). Figure 5 gives the soil and pile data obtained from post earthquake investigation of a recovered pile. Yoshida et al. (2007) collated many eyewitnesses statements and established the chronology of events of bridge failure. The bridge started to fail about 70 seconds after the first shock of the earthquake, i.e., long after the occurrence of the peak shock at 10s. The progressive collapse of the bridge took about 20 seconds, indicating that the inertia force cannot be the main cause of failure. The present numerical study thus ignores the inertia effect and a pseudo static analysis is carried out using the forces due to lateral spreading and superstructure load.

5.2 Details of the bridge

The Showa Bridge was a simple steel girder bridge crossing across the Shinano River, Japan. The bridge was 304m long, 24m wide with 12 spans (Fukuoka 1966). The foundation of each supporting pier was a single row of 9 tubular steel piles connected laterally by a pile cap (Figure 4). Each pile was 25m long with outer diameter of 0.609m. The wall thickness of the top 12m of the pile was 16mm and the bottom 13m was 9mm.

The axial load (P) carried by each pile from a dead load analysis was estimated by Bhattacharya (2003) as 740kN. The same axial load is taken in the present study. The design live loads are ignored as there was no significant traffic on the bridge during its failure. The axial load on each pile, after the bridge deck had fallen from the pile head is taken as half of the original axial load, i.e., 370kN.

Figure 6 shows the assumed stress-strain properties of SKK490 grade steel pile used in the Showa bridge. The yield strength σ_y and ultimate strength σ_u of the pile material is 315MPa

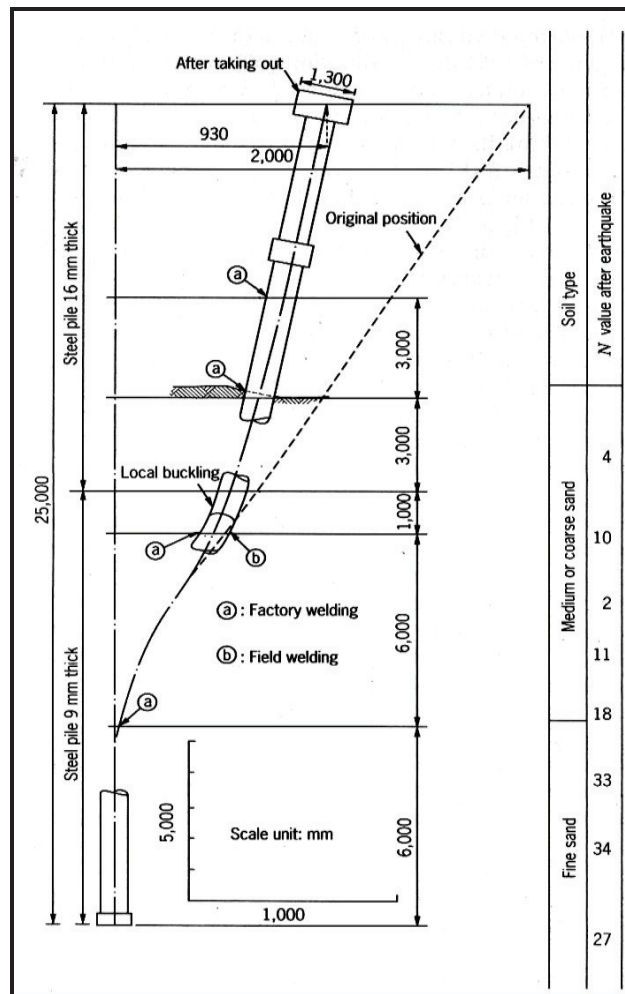


Figure 5. Details of one Showa Bridge pile after post earthquake recovery (Fukuoka, 1966).

and 490MPa respectively as per the Japanese standard ‘JIS-A:5525 Steel Pipe Piles’. The structural properties of the steel section at different axial loads are presented in Table 3.

5.3 Structural modelling of the bridge pile

The Showa bridge pile is modelled as a Beam on a Nonlinear Winkler Foundation (BNWF) using the finite element program SAP 2000 (CSI 2004). The 25m long pile was passing through a four-layer system of air, water, liquefied soil and non-liquefied soil (Figure 7). It was restrained over the bottom 6m, and was subjected to a combination of lateral and axial loads. The pile is modelled as a beam-column element and the soil-pile interaction is modelled as lateral soil springs ($p - y$ springs). The loading on pile can be considered in

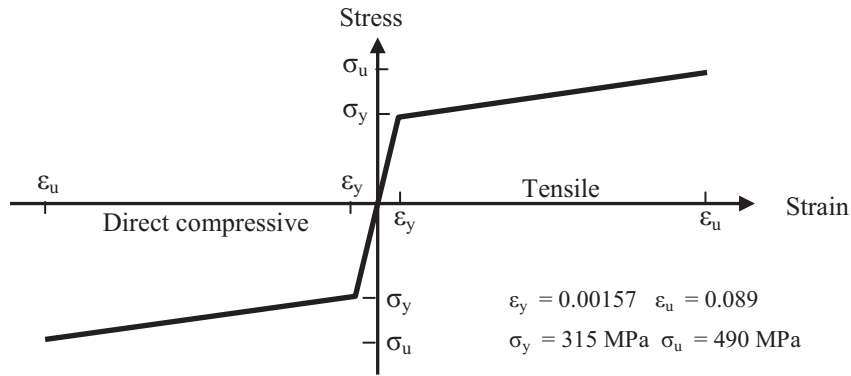


Figure 6. Stress-Strain relationship of pipe material used for Showa bridge pile.

Table 3. Structural properties of the Showa Bridge pile section

Sectional details of the pile	Axial Capacity (kN)	Bending Capacity (kNm)
	$t = 16\text{mm}$	$P_y = 9405$
		$P_u = 14630$
		$M_y = 1354$ (for $P = 0\text{kN}$) $= 1320$ (for $P = 370\text{kN}$) $= 1286$ (for $P = 740\text{kN}$)
		$M_p = 2675$ (for $P = 0\text{kN}$) $= 2442$ (for $P = 370\text{kN}$) $= 2415$ (for $P = 740\text{kN}$)
	$t = 9\text{mm}$	$P_y = 5355$
	$P_u = 8330$	$M_y = 790$ (for $P = 0\text{kN}$) $= 735$ (for $P = 370\text{kN}$) $= 680$ (for $P = 740\text{kN}$)
		$M_p = 1567$ (for $P = 0\text{kN}$) $= 1414$ (for $P = 370\text{kN}$) $= 1385$ (for $P = 740\text{kN}$)
<i>Note:</i> P_y = Yield capacity of pile in axial compression or tension P_u = Ultimate capacity of pile in axial compression or tension M_y = Yield moment capacity of pile M_p = Plastic moment capacity of pile		

either of the following two ways; a) applying the limiting pressure due to spreading soil, and b) applying the soil displacement at the free field ends of the $p - y$ springs (Figure 7). These two methods of loading can be referred to as force based pile loading and displacement based pile loading respectively. The strength of the $p - y$ springs are appropriately reduced when modelling liquefied soil. Details of these two types of pile loadings will be discussed in the following sections of this report.

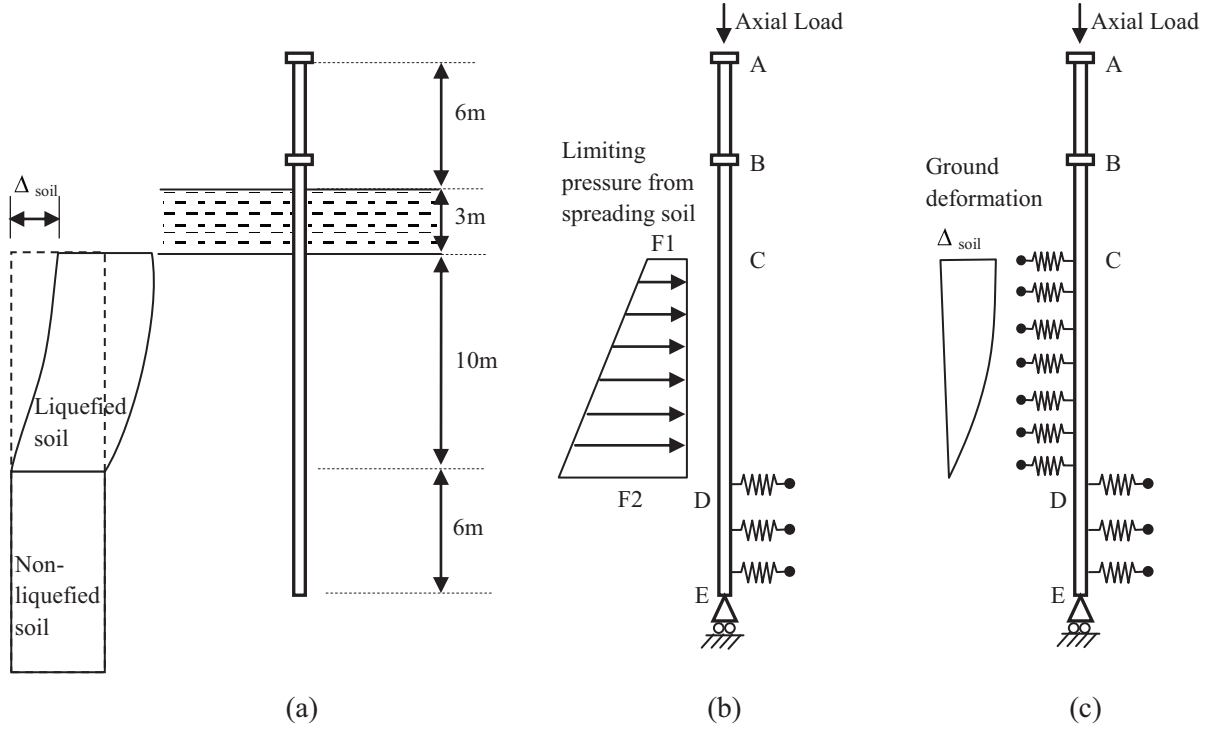


Figure 7. Pile subjected to lateral force from soil flow and axial load, a) field condition, b) force based model, c) displacement based model.

The deck section of the bridge were supported on piled bridge piers (Figure 4). The construction of the bridge was such that one end of the girder was fixed and the other end was free to slide longitudinally off the piers for the considered pile ‘P4’. Once the liquefaction starts, the pile head undergoes large displacement and the resistance offered from the bridge deck is limited and the pile head acts similar to free head. The present analytical model takes the boundary condition at pile head to be free. It is also assumed that the pile is stable at the base under vertical settlement, and hence, the pile tip is modelled as a roller support. These assumptions may not fully represent the field condition, however, changes in the boundary conditions at the pile tip do not have a significant effect on the bending-buckling interaction because of the large lateral restraint offered by the non-liquefied soil layer.

5.4 Soil model

The length of the pile in the liquefiable soil zone is about 10m (Figure 5) and the underlying denser non-liquefied sand layer (6m thick) can be assumed to provide restraint during lateral spreading. The nonlinear lateral soil spring properties (i.e., $p - y$ curves) are calcu-

Table 4. Lateral soil spring properties of bottom 6m soil surrounding the pile.

Depth from GL (m)	N	P_u (kN/m)	y_u (m)
11	18	24.40	0.02
12	33	100.1	0.02
13	33	225.1	0.02
14	34	399.4	0.02
15	34	623.1	0.02
16	34	896.1	0.02

Note: p_u = Maximum lateral resistance of soil, y_u = Maximum lateral mobilizing displacement of soil (see Figure 8), N = SPT blow count

lated according to the API guidelines (API 2000). The in-situ relative density (D_r) of the soil is calculated using equation 4 (Meyerhof 1957).

$$D_r = 21 \times \sqrt{\frac{N}{0.7 + \sigma'_v/98}} \quad (4)$$

where,

N = standard penetration test of the soil (see Figure 5)

σ'_v = effective overburden pressure in kPa at the depth of consideration

During liquefaction, the effective stress at the base of the liquefied soil layer becomes zero, and hence acts like a free surface. The submerged unit weight of soil is taken to be 10kN/m^3 . The estimated spring parameters for bottom 6m soil, the non-liquefied soil layer, are presented in Table 4. The $p - y$ spring for top 10m liquefied soil was calculated by multiplying the maximum lateral resistance (p_u) by a reduction factor, p-multiplier. The section 5.5.2 on displacement based analysis will discuss about the p-multiplier in detail. Figure 8 shows a typical $p - y$ spring as per API specifications.

5.5 Pile loading

The lateral loading on pile can either be a limiting force, or a ground displacement, as illustrated in Figure 7. In the Showa bridge case, the flow of top 10m liquefied soil was the only source of lateral force on pile, since the inertia effects are ignored (see section 5.1). The following sections will discuss the loading on the piles based on both the limiting force approach and the ground displacement approach.

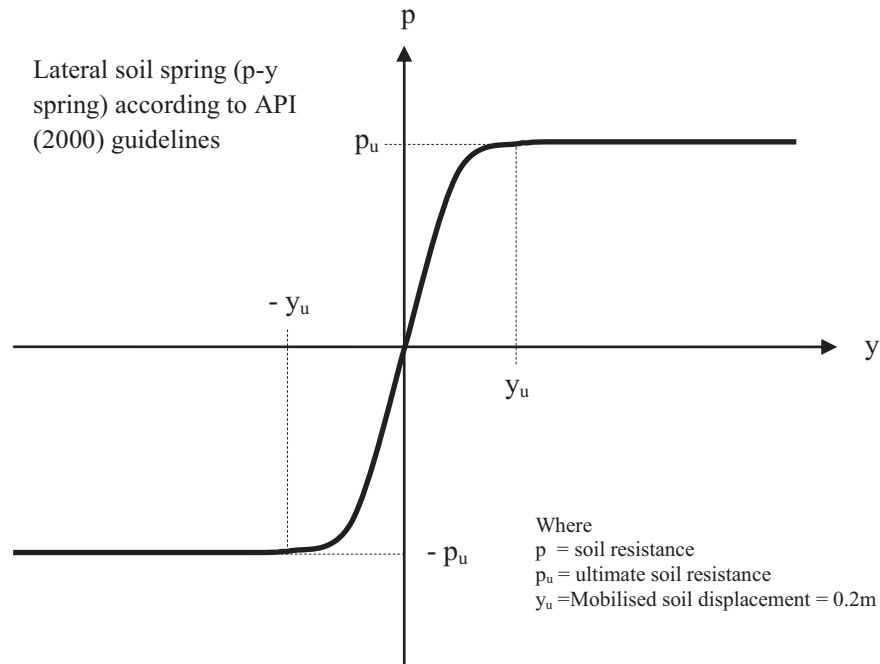


Figure 8. Nonlinear lateral soil spring ($p - y$ spring) used in the BNWF model.

5.5.1 Force based approach

As shown in Figure 7b, the lateral pressure on piles due to the flow of liquefied soils can be modelled as a limiting pressure on the pile. This way of defining the forces from soil flow is called force based approach. The Japanese Roads Association (JRA 2002) code is one of the modern codes of practice that specifies the limiting lateral pressure $F1$ and $F2$ (see Figure 7b) to be 30% of the total overburden pressure. Though, we know that the effective stress in liquefied soil is zero which may limit the strength and correspondingly flow pressure to be nearly zero, nothing has been addressed in JRA (2002) code. Hence, as per JRA (2002), the force on pile at the top of the liquefied soil layer, $F1$, is 30% of total overburden pressure due to water times the diameter of pile, i.e., $F1 = 0.3 \times 10\text{kN/m}^3 \times 3\text{m} \times 0.609\text{m} = 5.5\text{kN/m}$. Similarly, assuming the bulk unit weight of soil as 20kN/m^3 , $F2 = 0.3 \times (20\text{kN/m}^3 \times 10\text{m} + 10\text{kN/m}^3 \times 3\text{m}) \times 0.609\text{m} = 42\text{kN/m}$. He et al. (2006) also reported an experimental study which showed that the average lateral pressure from liquefied soil on a pile may vary from 20-40kPa (i.e., $F1$ and $F2$ may range between 20-40kPa). The present force based analysis considers three cases of lateral loading as shown in Figure 9.

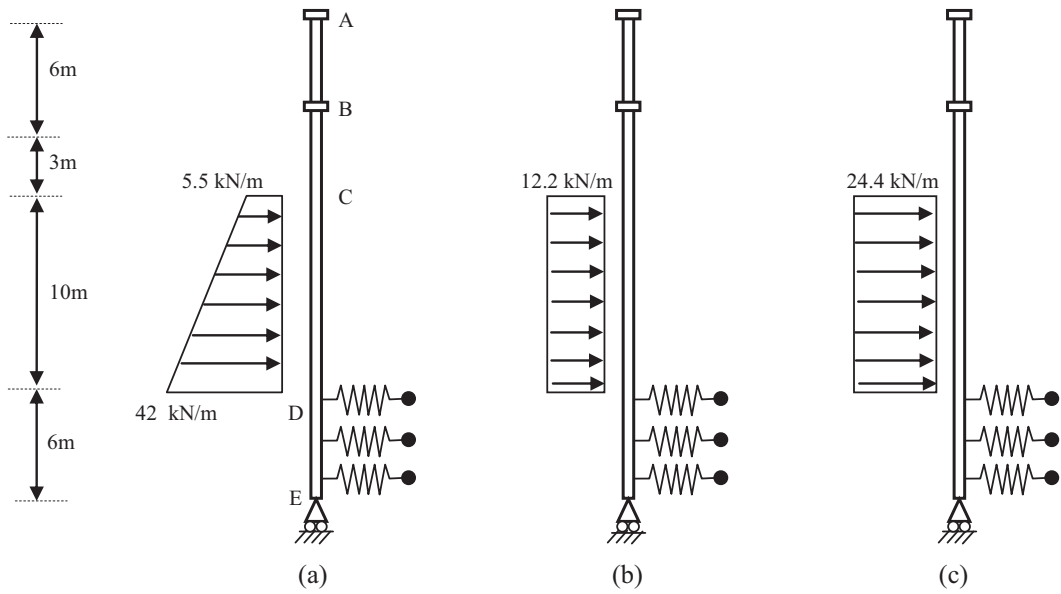


Figure 9. Pile subjected to lateral force from soil flow. a) JRA (1996) Loading b) He et al. (2006) lower bound loading of 20kPa c) He et al. (2006) upper bound loading of 40kPa.

5.5.2 Displacement based approach

Referring to Figure 7c, the lateral soil flow can also be modelled as finite displacements applied at the free ends of the $p - y$ springs. The $p - y$ springs of the liquefied soil is modelled as the $p - y$ springs of its non-liquefied state with a reduction factor, a p -multiplier. Though there are many literatures available which suggest p -multiplier values, still, there is no common consensus over it. Figure 10 shows some suggested p -multiplier values based on $(N_1)_{60}$ of the soils. In the present study, considering the average $(N_1)_{60}$ value of the liquefiable soil (Figure 5) as 10, the reduction factor according to AIJ (2001), Brandenburg (2005) and RTRI (1999) are 1/10, 1/50 and 1/1000 respectively. Research on this issue continues. These three cases of displacement based loading on pile are shown in Figure 11. The pattern of ground displacement with depth is assumed to be triangular. Other patterns such as rectangular or parabolic profile will give higher forces for the same ground displacement at surface. However, the scope of the present study does not require to check the pile response for different patterns of ground displacement.

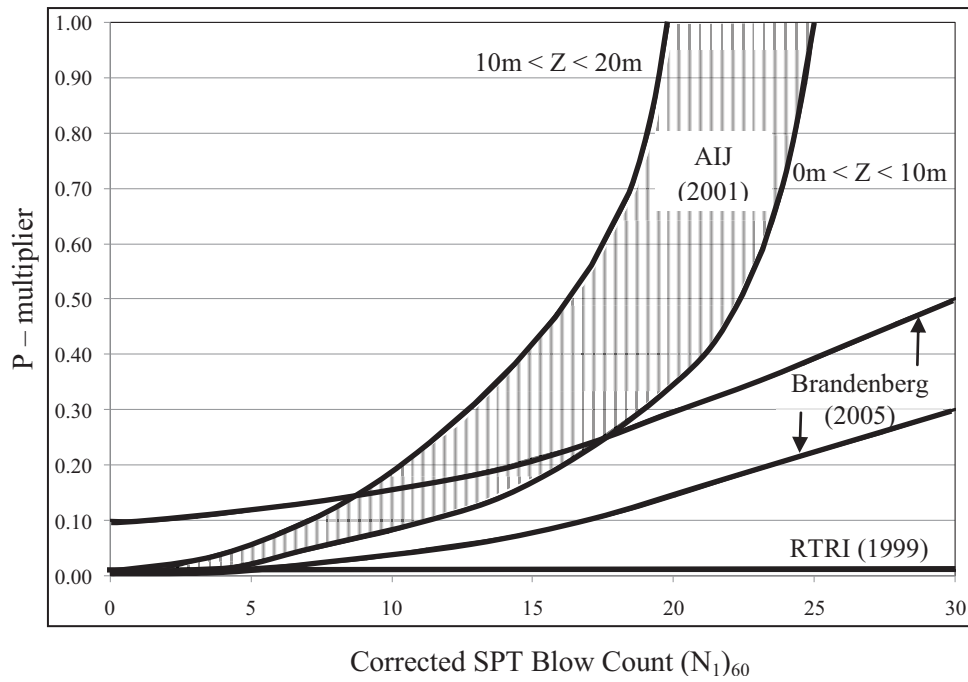


Figure 10. Reduction factor for p-y spring of liquefied soil.

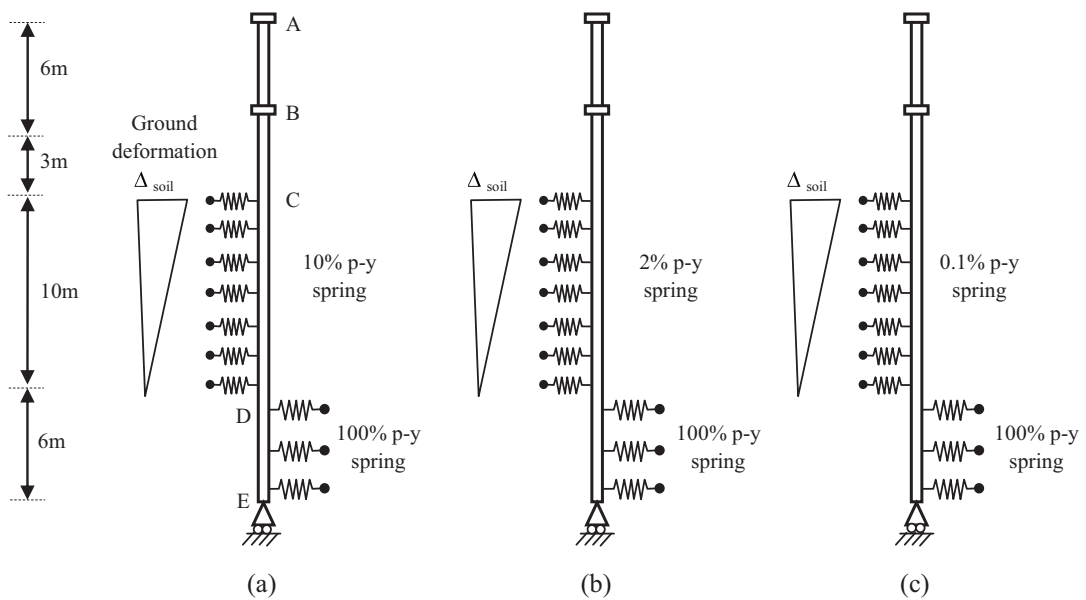


Figure 11. Pile subjected to ground displacement due to the flow of liquefied soil. (a) AIJ (2001) recommended soil parameters (b) Brandenburg (2005) recommended soil parameters (c) RTRI (1999) recommended soil parameters.

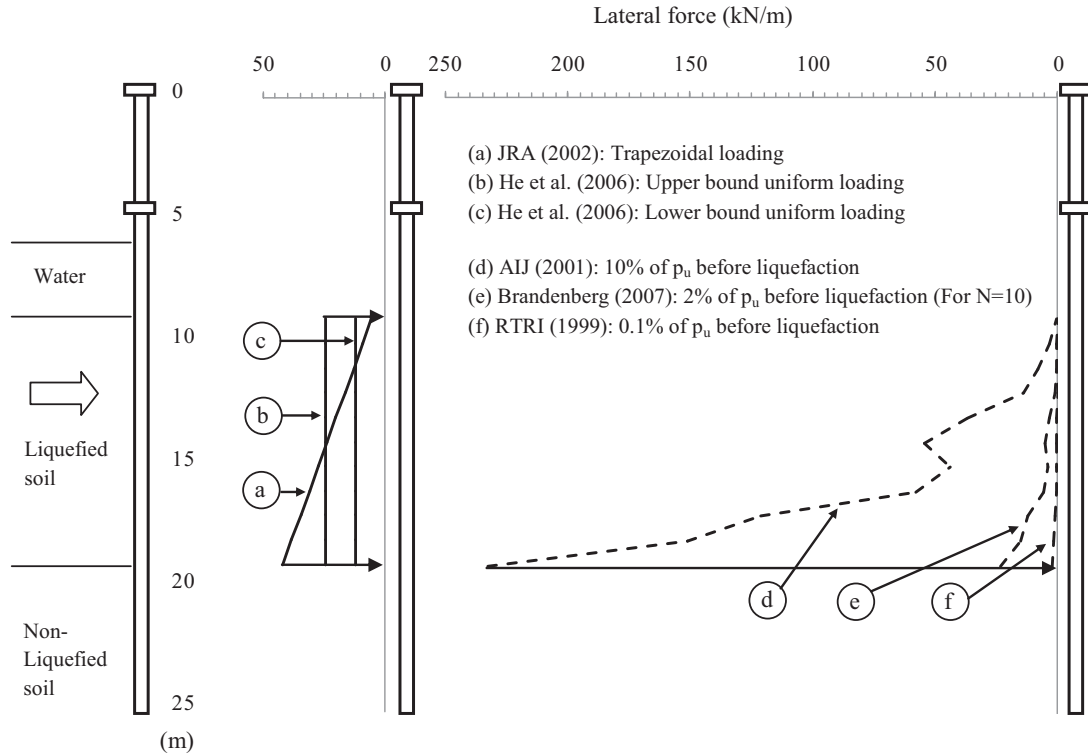


Figure 12. Lateral force on pile due to the flow of liquefied soil; force based approach versus displacement based approach (for p_u see Figure 8).

5.5.3 Force based approach versus displacement based approach

The actual lateral soil-pile interaction during the flow of liquefied soil is a complex behaviour. However, the above two methods simplify this by modelling the force from lateral movement of soil. Comparing the two methods, the force based analysis is simpler and can be done by hand calculations, but it is inadequate to model the actual behaviour of displacement profile of laterally spreading soil. On the other hand, the displacement based analysis is more representative of the process, compared with the force based analysis, but is best performed by a finite element program. The maximum lateral spreading forces the pile will be subjected to in the force and displacement based analyses are compared in Figure 12. The maximum load for displacement based analysis is taken as the ultimate load (p_u , in Figure 8) the $p - y$ spring will apply to the pile under large soil displacement. Figure 12 clearly demonstrates inconsistency in the magnitude of lateral force specified by different design guidelines and researchers.

5.6 Analysis type

The analysis of the present numerical model requires the following three conditions to be satisfied.

1. The axial load is present throughout the lateral loading phase, and the P-delta effect must be considered.
2. The load due to lateral spreading is gradual and proportional to the amount of soil flow, i.e., maximum ground displacement.
3. The analysis can be pseudo-static because the bridge failed after the earthquake ceased.

A nonlinear static analysis is carried out in SAP (CSI 2004). The loading function used in the analysis is shown in Figure 13. The pile is first subjected to the full axial load (P_{max}), and then the lateral pile load (either limiting pressure from soil flow(F_{max}) or ground displacement(Δ_{max})) is applied gradually keeping the axial load constant. The analysis includes P-delta and large displacement effects.

5.7 Results and discussion

5.7.1 Bending analysis

The BNWF model of the Showa Bridge pile (Figure 7) is analysed for six possible lateral loadings as presented in Figures 9 and 11. The first set of analysis ignores the effect of the axial load. From the force based analysis, Figure 14 plots the normalized pile head displacement (y/D) and normalized maximum bending moment (M/M_p) in pile against the amount of applied lateral force, where D and M_p are the diameter and plastic moment capacity of the pile. Similar results from displacement based analysis is presented in Figure 15. The normalized pile head deflection (y/D) and normalized maximum bending moment (M/M_p) are plotted against the ground displacement at the top of the liquefied soil layer (Δ_{soil}).

To compare the analysis results, the failure criterion of the pile is taken to be when the displacement of pile head is very large (say about $1D - 2D$) or the maximum bending

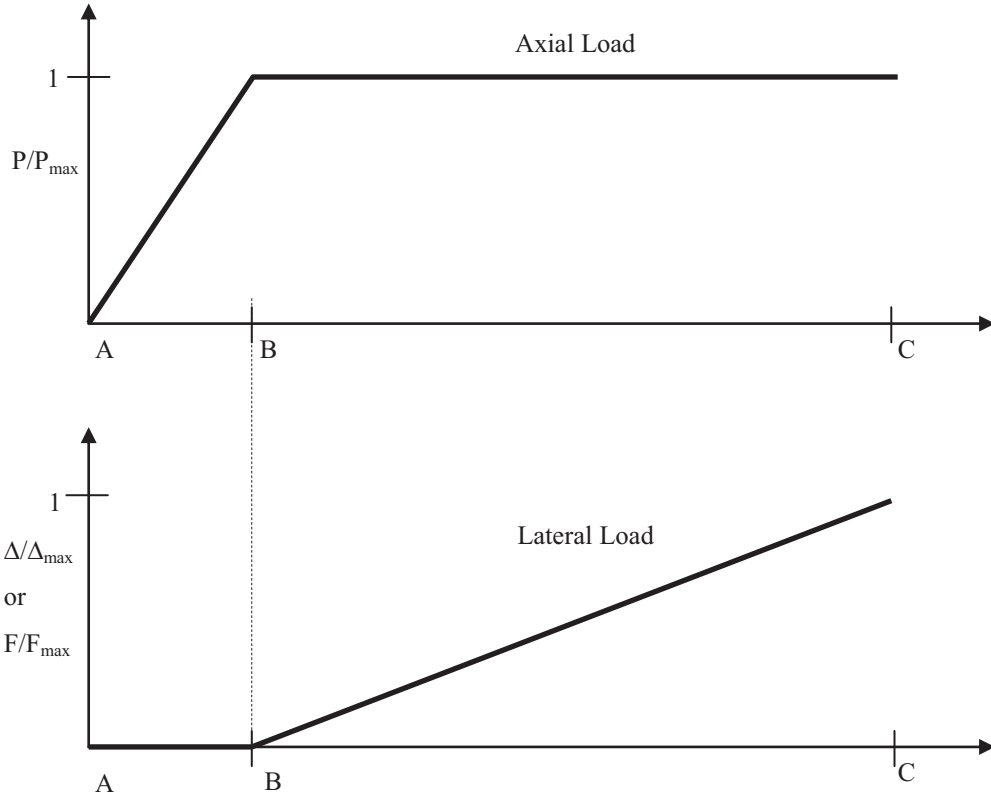


Figure 13. Loading function used in the analysis.

moment in pile is close to the plastic moment capacity ($M \approx M_p$). The results showed that two of the force based analysis cases and one displacement based analysis case predict failure of the pile when subjected to only bending (i.e., without considering the axial load). As expected, when the lateral load on the pile increases beyond yield, the pile deflects at a much faster rate. This is due to the fact that the stress-strain relationship (Figure 6) of the pile material is such that the stiffness of the material after yielding reduces about 100 times.

The upper bound lateral loading as suggested by He et al. (2006) predicts failure of the bridge pile at about 72% of loading (Figure 14), i.e., at a uniform pressure of 23.2kPa. The JRA loading also predicts failure at about 50% of its full load. Whereas, the lower bound value (i.e, $F = 20\text{kPa}$) do not predict failure. In addition, the JRA loading gives an intermediate estimate of pile response in the proposed range of lateral loading by He et al. (2006). Similar pile responses are also observed in one of the displacement based analysis cases (Figure 15). The displacement loading as per AIJ predicts failure, where the ultimate

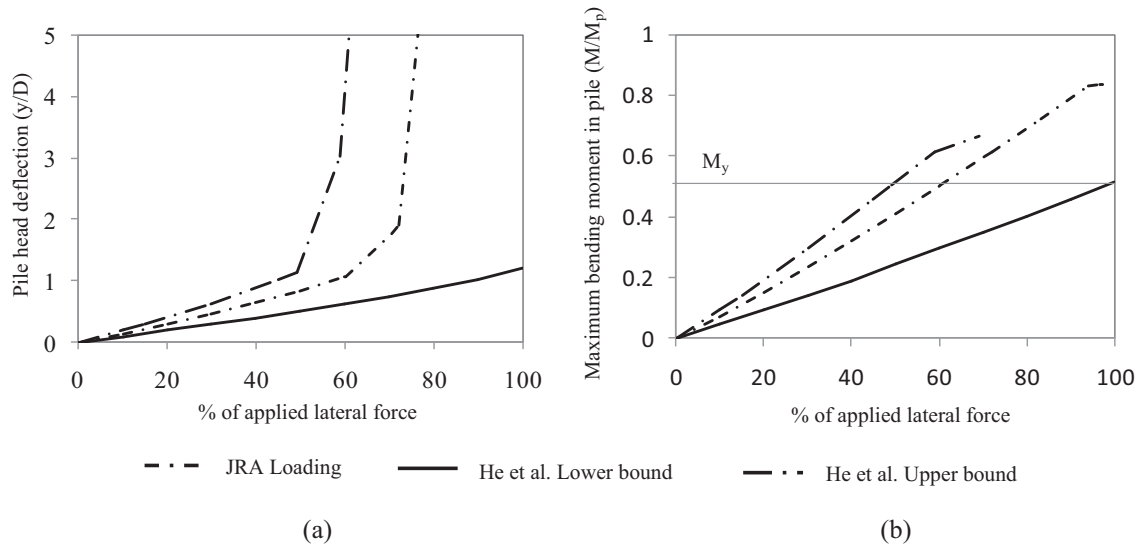


Figure 14. (a) Normalized pile head deflection and (b) normalized maximum bending moment in pile with increase in lateral loading.

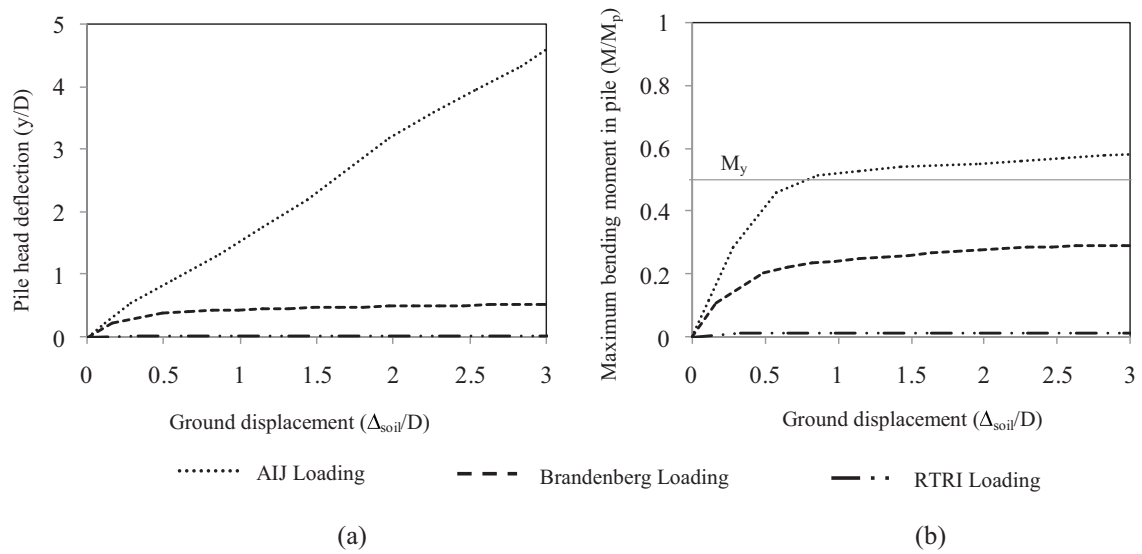


Figure 15. (a) Normalized pile head deflection and (b) normalized maximum bending moment in pile with increase in ground displacement.

lateral soil resistance, p_u , of the $p - y$ springs of liquefied soil is 10% of their non-liquefied p_u value. The Brandenburg (2005) loading and RTRI (1999) loading could not predict pile failure.

5.7.2 Buckling analysis

The Showa Bridge pile ($P4$) used in the present analysis is subjected to a dead load of 740kN as estimated by Bhattacharya et al. (2005). The length of pile in liquefiable soil zone is about 10m (Figure 5). Buckling calculation requires the unsupported length of the pile, L_0 , which is the combination of the length above ground level plus the depth of fixity (Figure 16). This is the standard procedure suggested by many codes of practice for evaluating unsupported pile length while calculating the bending moment in pile due to horizontal loads. As per Indian Standard IS-2911 (1979), the depth of fixity in service condition is estimated to be about 5D (Figure 16b), where D is the diameter of pile. At full liquefaction due to the earthquake, considering negligible lateral support from liquefied soil, the depth of fixity is about 4D (Figure 16c). Hence, the unsupported length of pile, which is about 12m ($9\text{m} + (5 \times 0.609\text{m})$) before liquefaction becomes 21.4m ($19\text{m} + (4 \times 0.609\text{m})$) at full liquefaction. Out of 21.4m of unsupported pile length, upper 13m is a 16mm tube and the lower 8.4m is a 9mm tube (see Figure 5). It is also clear from the deflected shape of the pile after earthquake (Figure 5) that the pile had a fixed-free boundary condition. The elastic buckling load (Euler buckling load), P_{cr} , of the considered pile can be estimated using the following equations for a column with two cross sections as suggested by Timoshenko and Gere (1961), section 2.14.

$$\frac{k_1}{k_2} = \tan k_1 l_1 \times \tan k_2 l_2 \quad (5)$$

where k_1 and k_2 are the buckling parameters as defined below.

$$k_1^2 = \frac{P_{cr}}{EI_1} \quad (6)$$

$$k_2^2 = \frac{P_{cr}}{EI_2} \quad (7)$$

On substituting $l_1 = 13\text{m}$, $l_2 = 8.5\text{m}$, $EI_1 = 275 \text{ MNm}^2$ and $EI_2 = 160 \text{ MNm}^2$, the solution for equation 5 gives the buckling load P_{cr} as 985kN. Hence, the factor of safety

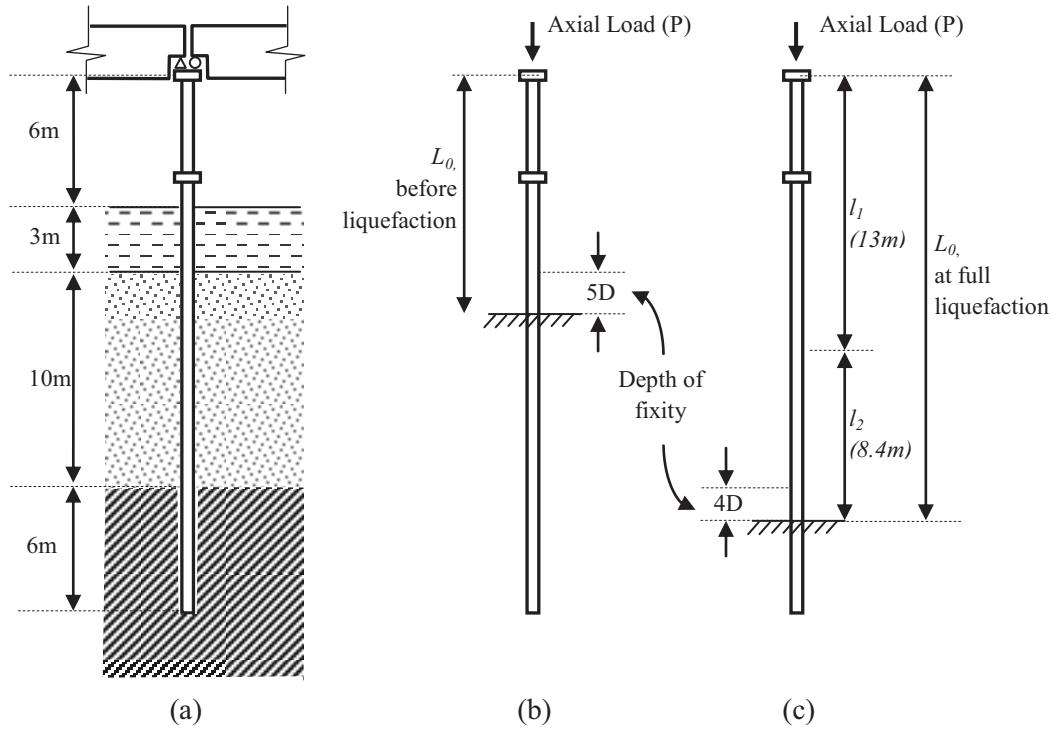


Figure 16. (a) Showa Bridge pile configuration, (b) Unsupported length (L_0) of pile before liquefaction, (c) Unsupported length (L_0) of pile at full liquefaction.

against Euler buckling is $P_{cr}/P = 985\text{kN}/740\text{kN} = 1.33$. Hence, if the buckling criterion is taken alone for design, the factor of safety is more than one suggesting that the pile can be treated safe. The dynamic amplification of the axial load during earthquake may reduce the factor of safety against buckling. However, this is not considered here as the inertia effects are ignored in the analysis (see section 5.1).

5.7.3 Bending-Buckling analysis

In the bending only analysis, three out of six analyses could not predict pile failure. Among these three analyses, one is from force based approach and two are from displacement based approach. Furthermore, the buckling analysis is also not able to describe the failure of the pile. Hence, one analysis from each approach of bending analysis is taken to study the effect of bending-buckling interaction.

The procedure described in the previous section was repeated for these two cases by incorporating three levels of axial load, 0kN, 370kN and 740kN (Table 5). In the force based approach, the He et al. (2006) lower bound loading is selected, and for the displacement

Table 5. Axial load combinations used in the analysis.

Axial load (P)	Remarks
0 kN	Analysis without axial load considerations. This would represent the simplified JRA (2002) procedure.
370 kN	The static load acting on the pile is half of the dead load. This may represent the condition when one deck has completely dislodged and the lateral flow of soil continues.
740 kN	The static dead load acting on the pile and any dynamic effects are ignored. This may represent a situation where the earthquake has stopped but the soil is fully liquefied and is flowing laterally past the pile. The bridge deck is still intact.

based approach, the Brandenburg (2005) loading was used.

Figure 17 plots the normalized pile head displacement (y/D) against normalized maximum bending moment in pile (M/M_p) with respect to the amount of lateral load. Similar results for displacement based analysis are plotted in Figure 18 against the maximum ground displacement (Δ_{soil}). For a lateral pressure of 20kPa (i.e, He et al. (2006) lower bound value), which could not predict failure when no axial load was applied, predicts failure when the axial loads are incorporated in the analysis. The pile fails at 60% of the lateral load when an axial load of 370kN is used. This reduces further to only about 11% when full axial load of 740kN is applied.

For the Brandenburg (2005) lateral loading case, with no axial load, the lateral ground displacement imposes a maximum pile head displacement of about 0.5m. At peak ground displacement (Δ_{soil}) of about 0.6m, the whole 10m liquefied soil column fully mobilizes and applies a constant pressure equal to the limiting pressure (Figure 18). Hence, beyond 0.6m of maximum ground displacement, the deformation and bending moment in the pile remains constant for increasing ground displacement. When the axial load is included in the analysis, the pile head suddenly becomes unstable (represented by the sharp increase in slope of the curve as seen in Figure 18) at a lower ground displacement. This sharp increase corresponds to the post-yield behaviour of pile.

For an axial load of 370kN, corresponding to half the weight of the deck, the pile do not yield. However, when the full dead weight of the superstructure is applied the analysis

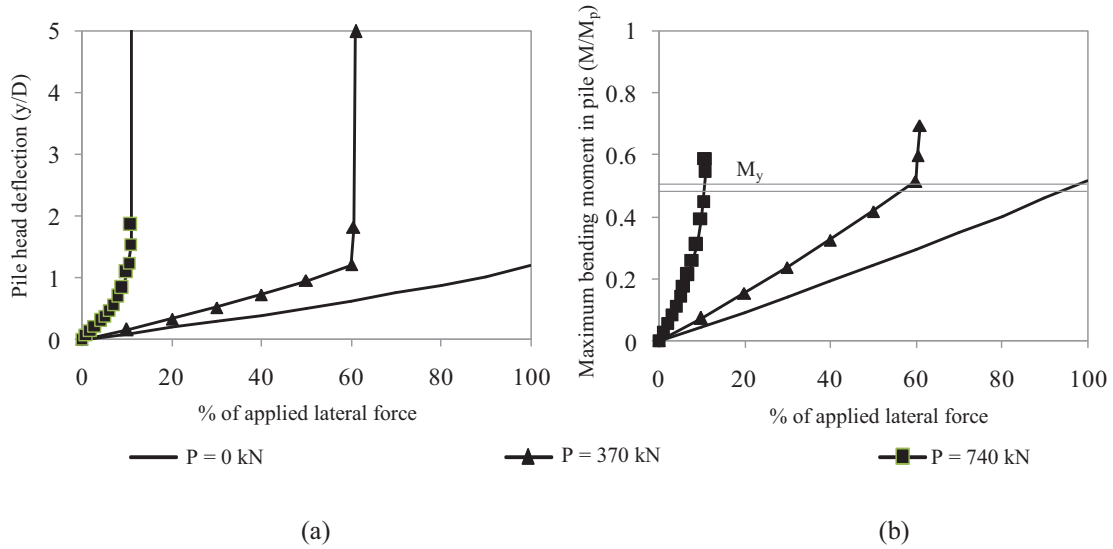


Figure 17. (a) Normalized pile head displacement and (b) normalized maximum bending moment in pile with respect to lateral force for $P = 0\text{kN}$, 370kN and 740kN .

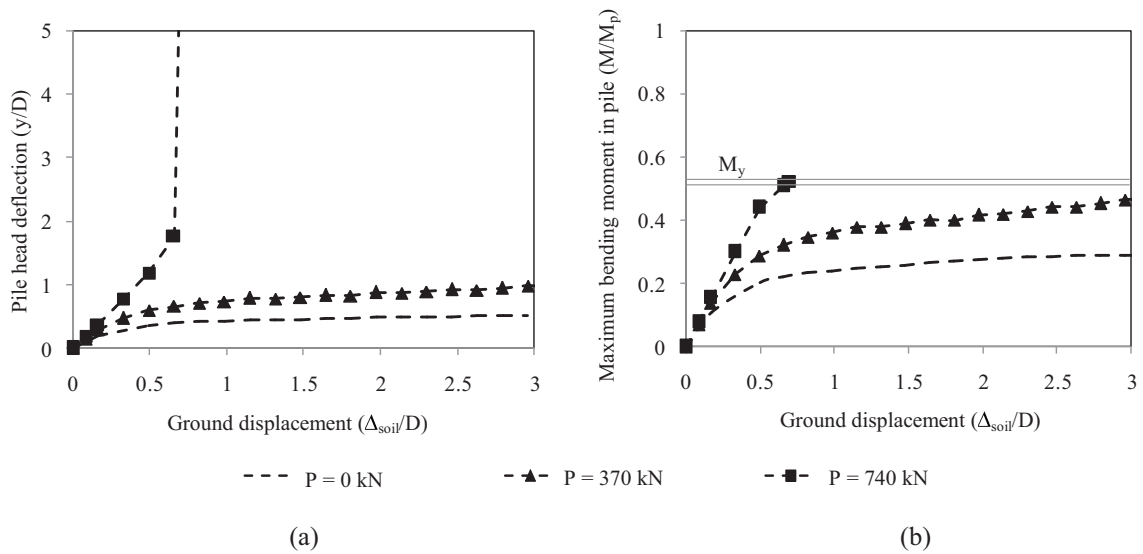


Figure 18. (a) Normalized pile head displacement and (b) normalized maximum bending moment in pile with increase in ground displacement for $P = 0\text{kN}$, 370kN and 740kN .

predicts failure. The analysis also showed that for the same lateral loading, the deflection and bending moment in the pile increases with an increase in axial load.

5.8 Remarks on results

Three cases of loading in the present analysis showed that the pile is safe while subjected to lateral spreading force alone. Also, the buckling analysis have shown that the factor

of safety of the pile against Euler buckling is about 1.33. This indicates that, if the pile will be designed for bending and buckling criteria in isolation, it can be considered safe. However, the pile can be seen to fail when the combined effect of lateral and axial load (i.e., bending-buckling interaction) is taken into account along with lateral spreading. Hence, designers must therefore consider the bending-buckling interaction during seismic design of pile foundations in liquefiable soils. Though the exercise shows the significance of bending buckling interaction for piles in liquefiable soil, the actual cause of Showa Bridge failure or the actual cause of pile collapse may be due to a combination of various effects which is beyond the scope of this study.

6 Conclusion

The following conclusions can be drawn from the present study:-

1. The current understanding of the pile failure in liquefiable soils considers either bending or buckling as a probable cause of failure. However, in reality, the two mechanisms interact. Hence, the pile foundations designed with these mechanisms separately might become un-conservative when the mechanisms interact.
2. Case studies of the seismic performance of pile foundations have shown that bending-buckling interaction can be a major failure mechanism for pile foundations in seismically liquefiable ground.
3. The design value of lateral load on piles due to the flow of liquefied soil varies widely according to various design guidelines used. Further research is required to arrive at more precise quantification of this lateral loading.
4. The analyses showed that 3 out of 6 models of lateral spreading analysis did not predict failure when analyzed using the conventional bending analysis method. The pile is also considered safe against Euler buckling with a safety factor of 1.33. Analyses, however, that do not show failure under bending alone can predict failure when bending-buckling interaction is taken into account.
5. It is important for the designers to take into account the bending-buckling interaction during seismic design of piles in liquefiable soils.

7 References

- Abdoun, T. and Dobry, R. (2002). “Evaluation of pile foundation response to lateral spreading.” *Soil Dynamics and Earthquake Engineering*, 22(9-12), 1051–1058.
- AIJ (2001). “Recommendations for design of building foundations.” Architectural Institute of Japan. (In Japanese).
- API (2000). “2A (WSD).” *Recommended Practice for Planning, Designing, and Constructing Fixed Offshore Platforms-Working Stress Design. Version 21st.*
- Berrill, J. B., Christensen, S. A., Keenan, R. P., Okada, W., and Pettinga, J. R. (2001). “Case study of lateral spreading forces on a piled foundation.” *Geotechnique*, 51(6), 501–517.
- Bhattacharya, S. (2003). “Pile instability during earthquake liquefaction,” Phd thesis, University of Cambridge, UK.
- Bhattacharya, S., Blakeborough, A., and Dash, S. R. (2008). “Learning from collapse of piles in liquefiable soils.” *Civil Engineering, Proceedings of Institution of Civil Engineers (ICE)*, 161(Special Issue 2), 54–60.
- Bhattacharya, S., Bolton, M. D., and Madabhushi, S. P. G. (2005). “A reconsideration of the safety of the piled bridge foundations in liquefiable soils.” *Soils and foundations*, 45(4), 13–26.
- Bhattacharya, S. and Madabhushi, S. P. G. (2008). “A critical review of methods for pile design in seismically liquefiable soils.” *Bulletin of Earthquake Engineering*, 6(3).
- Bhattacharya, S., Madabhushi, S. P. G., and Bolton, M. D. (2004). “An alternative mechanism of pile failure in liquefiable deposits during earthquakes.” *Geotechnique*, 54(3), 203–213.
- Brandenberg, S. J. (2005). “Behavior of pile foundations in liquefied and laterally spreading ground,” Phd thesis, Univ. of California at Davis, Davis, California.
- CSI (2004). “Sap 2000: V11.0 - integrated software for structural analysis and design..” Computer and Structures Inc (CSI), Berkeley, California, USA.
- Dash, S., Govindaraju, L., and Bhattacharya, S. (2009). “A case study of damages of the Kandla Port and Customs Office tower supported on a mat-pile foundation in liquefied soils under the 2001 Bhuj earthquake.” *Soil Dynamics and Earthquake Engineering*, 29(2),

333–346.

- Dash, S. R. and Bhattacharya, S. (2007). “Criteria for design of piled foundations in seismically liquefiable deposits.” *Proceedings, 4th International Conference on Earthquake Geotechnical Engineering*, (Paper.1724).
- Dobry, R. and Abdoun, T. (2001). “Recent Studies on Seismic Centrifuge Modeling of Liquefaction and Its Effect on Deep Foundations.” *Proceedings, Fourth International Conference on Recent Advances in Geotechnical Earthquake Engineering and Soil Dynamics, San Diego*, 1–30.
- Eurocode (1998). “Design provisions for earthquake resistance of structures- foundations, retaining structures and geotechnical aspects.” En 1998-5:2004 edition.
- Finn, W. D. L. and Fujita, N. (2002). “Piles in liquefiable soils: seismic analysis and design issues.” *Soil Dynamics and Earthquake Engineering*, 22(9-12), 731–742.
- Fukuoka, M. (1966). “Damage to civil engineering structures.” *Soils and foundations*, 6(2), 45–52.
- Goh, S. and O’Rourke, T. D. (1999). “Limit state model for soil–pile interaction during lateral spread.” *Proc. 7th US–Japan Workshop on Earthquake Resistant Design of Lifeline Facilities and Countermeasures Against Soil Liquefaction, Seattle*, 237–260.
- Hamada, M. (1992a). “Large ground deformations and their effects on lifelines: 1964 Niigata earthquake. Case studies of liquefaction and lifelines performance during past earthquake.” *Technical Rep. NCEER-92-0001, National Center for Earthquake Engineering Research, Buffalo, NY*, 3–1.
- Hamada, M. (1992b). “Large ground deformations and their effects on lifelines: 1983 Nihonkai-Chubu earthquake. Case studies of liquefaction and lifelines performance during past earthquake.” *Technical Rep. NCEER-92-0001, National Center for Earthquake Engineering Research, Buffalo, NY*, 4–1.
- Hamada, M. (2000). “Performance of foundations against liquefaction-induced permanent ground displacement..” *Proc. of 12th World Conf. on Earthquake Engineering*, 1754–1761.
- He, L., Elgamal, A., Abdoun, T., Abe, A., Dobry, R., Meneses, J., Sato, M., and Tokimatsu, K. (2006). “Lateral load on piles due to liquefaction-induced lateral spreading during one-g

- shake table experiments.” *100th Anniversary Earthquake Conference, USA*.
- IS-1893 (2000). “Part-1: Criteria for earthquake resistant design of structures..” Bureau of Indian Standard (New Delhi).
- IS-2911 (1979). “Part-1/sec-1: Criteria for earthquake resistant design of structures..” Bureau of Indian Standard (New Delhi).
- Ishihara, K. (1993). “Liquefaction and flow failure during earthquakes.” *Geotechnique*, 43(3), 351–415.
- Ishihara, K. (1997). “Terzaghi oration: geotechnical aspects of the 1995 Kobe earthquake.” *Proceedings of 14th International Conference on Soil Mechanics and Foundation Engineering, Hamburg*, 4, 2047–2073.
- Iwasaki, T. (1984). “A case history of bridge performance during earthquakes in Japan.” *Keynote lecture at the International Conference on Case histories in Geotechnical Engineering, University of Missouri Rolla*. Shamsheer Prakash (edt).
- JRA (2002). “Specification for highway bridges, part v-seismic design.
- Kimura, Y. and Tokimatsu, K. (2005). “Buckling Stress of Steel Pile with Vertical Load in Liquefied Soil.” *Journal of Structural and Construction Engineering*, 73–78.
- Knappett, J. A. and Madabhushi, S. P. G. (2005). “Modelling of Liquefaction-Induced Instability in Pile Groups.” *Seismic Performance and Simulation of Pile Foundations in Liquefied and Laterally Spreading Ground (Geotechnical Special Publication (GSP) No. 145)(eds. RW Boulanger and K. Tokimatsu), American Society of Civil Engineers, Reston, VA, USA*, 225–267.
- Kramer, S. (1996). “Geotechnical earthquake engineering.” *Prentice-Hall Civil Engineering and Engineering Mechanics Series, Upper Saddle River, NJ: Prentice Hall,— c1996*.
- Meyerhof, G. G. (1957). “Discussion on soil properties and their measurement.” *Proceedings of the Fourth International Conference on Soil Mechanics and Foundation Engineering*, Discussion 2, Vol.III.
- NEHRP (2000). “Seismic regulations for new buildings and other structures..” Commentary for Federal Emergency Management Agency, fema-369 edition.
- NISEE. “National Information Services for Earthquake Engineering.

- Rollins, K., Gerber, T., Lane, J., and Ashford, S. (2005). “Lateral resistance of a full-scale pile group in liquefied sand.” *Journal of Geotechnical and Geoenvironmental Engineering*, 131, 115.
- RTRI (1999). “Design standard for railway facilities-seismic design.” Railway Technical Research Institute. in Japanese.
- Shanker, K., Basudhar, P., and Patra, N. (2007). “Buckling of Piles under Liquefied Soil Conditions.” *Geotechnical and Geological Engineering*, 25(3), 303–313.
- Soga, K. (1997). “Geotechnical aspects of Kobe earthquake.” *EEFIT Report*.
- Takahashi, A. (2002). “Soil-pile-interaction in liq-uefaction induced lateral spreading of soils,” PhD thesis, Tokyo Institute of Technology, Japan.
- Takata, T., Tada, Y., Toshida, I., and Kuribayashi, E. (1965). “Damage to bridges in Niigata earthquake.” *Report no-125*, 5.
- Timoshenko, S. P. and Gere, J. M. (1961). *Theory of elastic stability*. McGraw Hill book company, New York, USA.
- Tokimatsu, K., Hiroshi, O. O., Satake, K., Shamoto, Y., and Asaka, Y. (1998). “Effects of lateral ground movements on failure patterns of piles in the 1995 Hyogoken-Nambu earthquake.” *Proceedings of a speciality conference, Geotechnical Earthquake Engineering and Soil Dynamics III, ASCE Geotechnical Special Publication*, 1175–1186.
- Tokimatsu, K., Mizuno, H., and Kakurai, M. (1996). “Building damage associated with geotechnical problems.” *Soils and foundations*, 219–234.
- Tokimatsu, K. and Suzuki, H. (2005). “Effect of inertial and kinematic interactions on seismic behaviour of pile foundations based on large shaking table tests.” *Proceedings of the 2nd CUEE conference on urban earthquake engineering*.
- Tokimatsu, K., Suzuki, H., and Sato, M. (2005). “Effects of dynamic soil-pile structure interaction on pile stresses.” *J Struct Const Eng*, (587), 125–132.
- Wilson, D., California, for Geotechnical Modeling, C., and of Transportation, D. (1998). *Soil-pile-superstructure interaction in liquefying sand and soft clay*. University of California, Davis.
- Yasuda, S., Yoshida, N., Kiku, H., Adachi, K., and Gose, S. (1999). “A simplified method

to evaluate liquefaction-induced deformation.” *Earthquake Geotechnical Engineering. Rotterdam: Balkema*, 555–560.

Yoshida, N., Tazoh, T., Wakamatsu, K., Yasuda, S., Towhata, I., Nakazawa, H., and Kiku, H. (2007). “Causes of Showa Bridge Collapse in the 1964 Niigata Earthquake Based on Eyewitness Testimony.” *Soils and Foundations*, 47(6), 1075.